Developmental Biology 351 (2011) 1–12

Contents lists available at ScienceDirect

Developmental Biology

journal homepage: www.elsevier.com/developmentalbiology

Experimental Sey mouse chimeras reveal the developmental deficiencies of Pax6-null granule cells in the postnatal cerebellum

Douglas J. Swanson *, Dan Goldowitz

Centre for Molecular Medicine and Therapeutics, Department of Medical Genetics, University of British Columbia, 950 West 28th Ave, Vancouver, Canada BC V5Z 4H4

ARTICLE INFO

Article history:
Received for publication 3 August 2010
Revised 6 November 2010
Accepted 10 November 2010
Available online 29 November 2010

Keywords:
External germinal layer (EGL)
Migration
Differentiation
Foliation
Radial glia
Purkinje cell

ABSTRACT

Pax6 has been implicated in cerebellar granule cell development, however the neonatal lethality of the Sey/Sey mutant has precluded a more detailed study of this late developing neuronal type. In this study we use experimental mouse chimeras made from wildtype and Pax6-null embryos to circumvent early lethality and assess the developmental potential of mutant cells in the construction of the cerebellum. We have identified the granule cell as a direct target of mutant gene action, with glia and Purkinje cells being affected in what is largely a non-cell autonomous manner.

Most dramatically, in postnatal day 21 (P21) chimeras, mutant cells are largely absent in the anterior and posterior cerebellum while present in central lobules, but amidst disorganized cerebellar architecture. Analysis of P0/1 and P10 chimeras demonstrates a profound temporally based defect where mutant cells colonize the anterior and posterior EGL but fail to migrate to the IGL. Mutant granule cells in the central lobules can reach the IGL in an abnormal manner, with large streams of cells forming raphes through the molecular layer.

These studies provide new insights into the role of Pax6 in postnatal cerebellar development that pinpoint the granule cell as an intrinsic target of the mutant gene and key events in the life of the developing granule cell that depend upon normal Pax6 expression.

Introduction

The paired-box homeodomain transcription factor Pax6 has been shown to be a key regulatory gene for the development of several regions of the CNS, including the eye and retina, the spinal cord, the forebrain, and cerebellum (Engelkamp et al., 1999; Ericson, et al., 1997; Grindley et al., 1995; Hill et al., 1991; Schmahl, et al., 1993; Swanson et al., 2005; Takahashi and Osumi, 2002). In the developing cerebellum, this gene is expressed in the proximal neurepithelium, the rhombic lip and granule cell progenitors (Fink et al., 2006; Walther and Gruss, 1991; Swanson, unpublished results). In the Sey embryo, cerebellar granule cell progenitors have multiple phenotypes, including a delay in tangential migration, disorganization of granule cell precursors in the EGL, and disruption of parallel fiber initiation (Engelkamp, et al., 1999; Swanson et al., 2005; Yamasaki, et al., 2001). The readout of these developmental abnormalities and the full developmental potential of the Pax6-null granule cell is not accessible due to the neonatal lethality of the Pax6 mutation. One means to circumvent this lethality is to examine the development of the cerebellum in organotypic slice or dissociate cell culture (Engelkamp et al., 1999; Swanson et al, 2005). Engelkamp et al. (1999) showed exuberant migration of granule cells from EGL explants in culture, while Swanson et al. (2005) found a marked aggregation of Pax6-null cells in dissociate cultures. In addition, granule cells retained an immature phenotype as indicated by enhanced proliferation and incomplete differentiation. While culture models have their benefits, these systems allow for only a limited view of development and under conditions where the normal developmental milieu and cellular relationships are disrupted. We have adopted an experimental mouse chimera approach in order to extend the time frame for examining the capabilities Pax6-null cells in an in vivo developmental setting.

In our analysis of Pax6-null<->wildtype chimeras, using cell markers for both genotypes of cells, we find Pax6-null granule cells are dramatically deficient in initiating folia formation, competing with wildtype cells in tangential and radial migration, and subsequent colonizing the internal granule cell layer of the cerebellum. This is most parsimoniously seen as a granule cell intrinsic defect with other abnormalities in the Pax6-null cerebellum likely secondary to what appears to be a defect involving developmental timing.

Materials and methods

Animal care and breeding

Two strains of mice possessing different Pax6-null alleles were employed in generating experimental chimeras, the Pax6^{Sey} strain

* Corresponding author. Fax: +1 604 875 3018.
E-mail address: djswan@cmmt.ubc.ca (D.J. Swanson).

0012-1606/$ – see front matter © 2010 Elsevier Inc. All rights reserved.
doi:10.1016/j.ydbio.2010.11.018

(obtained from Robert Grainger and Marilyn Fisher, University of Virginia, maintained on a mixed genetic background) and the Pax6$^{Sey\text{-}Neu}$ strain [obtained from Brigid Hogan, Duke University, maintained on an ICR background, (Grindley et al., 1997)]. The Pax6$^{Sey\text{-}Neu}$ strain was crossed to a GFP transgenic reporter line [chick β-actin:GFP maintained on an ICR background (Hadjantonakis et al., 2002)] to generate the Pax6^{NGFP} line that provides a constitutively expressed GFP marker for cells derived from the Pax6-null embryos. In some cases we also used Pax6^{Sey} mice carrying β-galactosidase inserted into the Math1 locus (thus Pax6$^{+/Sey}$-Math1$^{+/\beta\text{-}Gal}$). These mice were generated by crossing the Pax6^{Sey} strain to Math1$^{+/\beta\text{-}Gal/+}$ mice [obtained from Huda Zoghbi, Baylor College of Medicine; (Bermingham et al., 1999)]. Mice heterozygous for the Math1$^{\beta\text{-}Gal/+}$ allele are normal with respect to cerebellar development (Ben-Arie et al., 1997; Jensen et al., 2002). For the wild-type component of experimental chimeras we used Rosa26 (Friedrich and Soriano, 1991), Balb/cJ, or FVB/N-GFP mice (a transgenic mouse strain carrying EGFP expression under control of chicken beta-actin promoter) (D. Goldowitz unpublished). Efforts were made to minimize animal suffering and to reduce the number of animals used, and all studies were conducted in accordance with University of Tennessee, NIH, and Society for Neuroscience policies on the ethical use of animals in research.

Aggregation chimeras

Experimental mouse chimeras were generated as described previously (Goldowitz and Mullen, 1982; Goldowitz, 1989). Four- to eight-cell embryos from the mutant strain (Pax6$^{+/+}$, Pax6$^{+/-}$ or Pax6$^{-/-}$) were cultured overnight together with wild-type embryos. After successful fusion, blastocysts were transplanted into the uterine horn of pseudo-pregnant host ICR females. A Pax6^{Sey} x Pax6^{NGFP} cross was used to generate Pax6-null (*Sey/Sey-Neu*) embryos carrying the GFP marker for the mutant component of the chimeras. Most chimeras were made using Rosa26 embryos as the wild-type component providing a β-galactosidase marker in all wild-type cells. Percent chimerism was estimated from tail or liver expression of GFP fluorescence (Sey cells) and/or β-galactosidase activity (wildtype cells). The genotype of the Sey component (*+/+*, *Sey/+*, *Sey^{Neu}/+*, and *Sey/Sey^{Neu}*) was determined using a mutagenically separated PCR technique (MS-PCR; [47]) as previously detailed (Swanson et al., 2005). We identified and phenotypically assessed 25 Sey/Sey^{Neu} mutant chimeras out of a total of 224 live chimeras [P0.5–1.5, 16/43 (37%); P10.5–P15.5, 6/132 (<5%); P22.5–23.5, 3/49 (6%)].

Histological methods

All animals were prepared for transcardiac perfusion using PBS and 4% paraformaldehyde under deep Avertin anesthesia. Tissues were post-fixed *in situ* for 2 hrs in fix. The brains were dissected out of the skull and stored at 4 °C in PBS (0.1 M, containing 0.02% Na Azide) until processing. Tissues were cryoprotected in 30% sucrose in PBS overnight and serially cryosectioned at 12–16 μm.

When appropriate, serial sections from brains and liver were stained for the presence of β-Gal activity using X-Gal (5-Bromo-4-chloro-3-indolyl-β-D-galactopyranoside) histochemistry as previously described (Reiner et al., 2007). Tissue sections were counterstained with neutral red to highlight the cellular architecture.

Single-label immunofluorescence staining of chimera tissue was carried out as previously described (Swanson et al., 2005; Liu et al., 2007). Native GFP fluorescence was examined in comparison to immunofluorescent detection of cellular antigens with the following antibodies; anti-Pax6 (PRB-278P, rabbit, Covance, 1:500), to highlight wildtype granule cells and granule cell precursors; anti-GFAP (rabbit, 1:500, Dako) and anti-RC2 (mouse, 1:50, DSHB), for radial glial processes of both genotypes; anti-TuJ1 (MMS-435P, mouse, 1:500, Covance) and anti-Ki67 (clone SP6, mouse, 1:000, Thermo Scientific, Freemont, CA) for the determination of the differentiation status of granule cells; anti-calbindin D-28k (AB1778, rabbit, 1:500, Chemicon), for detection of Purkinje cell soma and dendrites; anti-β-Gal (CR7001RP, rabbit, 1:500, Cortex) for detection of β-Galactosidase expression driven from the Math1 locus in the Sey strain component of the chimeras (when these mice carried the Math1$^{\beta\text{-}Gal/+}$ allele) as noted in Fig. 8. The secondary antibodies used for these analyses were Goat anti-Rabbit whole IgG Alexa 594 conjugate (A11012, 1:1000) and Goat anti-mouse F(ab′)$_2$ Alexa 594 conjugate (A11020, 1:1000) (Molecular Probes/Invitrogen).

Analysis and photomicroscopy of brightfield histochemistry was performed with a Zeiss Axiophot microscope with the Axiocam/Axiovision hardware-software components (Carl Zeiss). Confocal microscopy was performed using either a BioRad confocal laser scanning microscope or an Olympus FV500 confocal laser scanning microscope and the FluoView image capture and analysis software.

Results

Survival and general observations in Sey/Sey^{Neu} chimeras

The homozygous Pax6-null mutation results in severe craniofacial malformations, a highly altered CNS, and subsequent post-parturitional death (Hogan et al., 1986). Of the 237 chimeras generated for this study, 25 had cellular contributions from homozygous mutant embryos (Table 1). The most profound phenotype in *Sey/Sey^{Neu}*<->wildtype chimeras was the rescue from immediate neonatal death that characterizes the Pax6-null pathology. Very high percentage mutant chimeras (estimated at 98–99%) did survive birth and showed craniofacial and ocular defects characteristic of the Pax6-null animal. In chimeras that ranged between 10% and 80% mutant cells we saw varying ocular defects that only roughly correlated with the donation of mutant cells to the embryo (Li et al., 2007). When there was a mismatch between percentage chimerism and phenotype, this was likely due to the method by which chimerism was assessed [i.e., from coat color and liver histochemistry (see Methods)]. In practice the percent chimerism readout from coat color and/or liver histochemistry may not always reflect the end product percent chimerism of nervous system

Table 1
Pax6-null Chimeras examined in present study.

Postnatal age	Chimera ID	Est. % chimerism[a]	Overt phenotype
0.5	1274	80	Disrupted eyes, No nares
0.5	1276	75	Disrupted eyes, Reduced nares
0.5	1310	90	na
0.5	1311	30	na
0.5	1313	40	na
0.5	1602	30	Disrupted eyes,
0.5	1603	70	Disrupted eyes
0.5	1604	99	Live Near Full Mutant
0.5	1698	med-high	One disrupted eye
0.5	1699	high	Live Near Full Mutant
0.5	1700	high	Live Near Full Mutant
0.5	1701	low	One disrupted eye
0.5	1865	high	Disrupted eyes, Reduced OlfBulbs
0.5	1867	med-high	Disrupted eyes, No OlfBulbs
1.5	1869	low	Small eyes, reduced OlfBulbs
1.5	1873	low	One disrupted eye, No OlfBulbs
10.5	1350	40–70	One disrupted eye, Reduced OlfBulb
10.5	1352	10	One disrupted eye
10.5	1624	60–80	na
10.5	1628	10–30	One disrupted eye
10.5	1741	55–80	Reduced OlfBulb
13.5	1325	na	na
22.5	1329	2–65	One disrupted eye
23.5	1281	40–60	Disrupted eyes
23.5	1295	30–60	Normal

na: not assessed.
[a] Based on estimates from coat color and tail/liver marker expression.

development. An example of this mismatch was seen in a low (10%) coat color chimera that expressed a severe cerebellar phenotype and unilateral ocular defect.

The overt phenotype of the P22–23 Sey/Sey^{Neu} chimeric cerebellum

The third postnatal week was examined as an age that reflects the morphology of an adult cerebellum. In the three Pax6-null chimeras assessed at this age, the overall size of mutant chimeric cerebella is visibly reduced and underdeveloped compared to control chimeras (Fig. 1). The folia are smaller than in controls, and a reduced complexity is most obvious in the central lobules. In the wild type cerebellum, lobules V-VIII are distinct with pronounced folial contours (Fig. 1A), while in the mutant chimeric cerebellum the foliation of these lobules is absent displaying a single smooth un-contoured lobule (bounded by arrowheads in Fig. 1C, E). The perturbations of the folial patterns are continued into the paravermis and cerebellar hemispheres (compare Fig. 1B with Fig. 1D, F). At the cellular level, abnormalities are most prominent in the granule cell population and manifested as a thinning of the IGL (highlighted by asterisks in Fig. 1D, C and detailed in Fig. 2F, H) and nests of ectopic granule cells below the pial surface (data not shown). The areas depleted of granule cells are sharply bounded by areas of relatively normal granule cell numbers (Fig. 2F, H). There are also some areas of Purkinje cell layer disorganization and these coincided with obvious disruptions of the granule cell population (asterisks in Fig. 2F, H).

Pax6-null cellular contribution to the P22–23 cerebellum

The contribution of wildtype and mutant cells to these areas of dysmorphology was examined using the β-Galactosidase and GFP reporter genes expressed in wildtype and mutant cells, respectively. There is a regional bias of Pax6-null granule cell contributions in mutant chimeras. In medial sections, the granule cells of the anterior and posterior lobules are predominantly wildtype (βGal-positive), with virtually no mutant granule cells (Fig. 1C, E and Fig. 2A, B). In contrast, the central lobules of the medial cerebellum, Pax6-null granule cells are more abundant; and it is these regions where structural anomalies occur

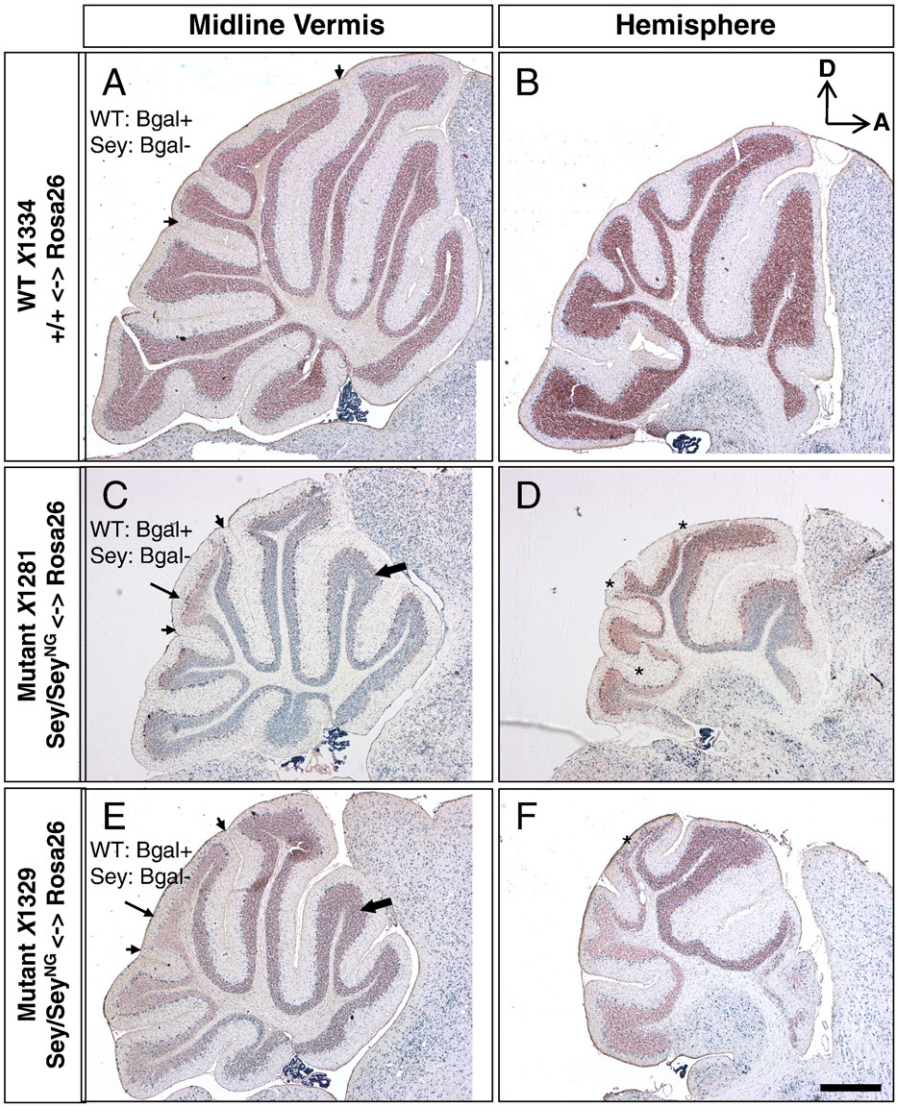

Fig. 1. P21 mutant chimeras show regional defects in cerebellar cytoarchitecture. (A–F) Medial vermis and the lateral hemisphere sections of cerebellum from a wildtype chimera (X1334, A, B) and two Pax6-null<->Rosa26 mutant chimeras (X1291; C, D and X1329 E, F) were stained for β-Gal activity and counterstained with neutral red. The mutant chimeras show smaller cerebella and noticeably under-foliated intermediate lobules in the vermis (arrowheads in A, C, and E designate the superficial boundaries of lobules V-VII affected in the mutants). Reduced β-Gal staining in the central lobules indicates the presence of Pax6-null granule cells in the IGL (β-Gal-negative, thin arrows in C and E; depicted in GFP epifluorescence in Fig. 2C and D) and very few mutant granule cells in the anterior lobules (thick arrows in C and E; depicted in GFP epifluorescence in Fig. 2A and B). Disturbances in the cytoarchitecture are highlighted by regions of cell loss and degeneration (Asterisks in D and F). Orientation arrows point dorsal (D) and anterior (A). Scale Bar = 500 μm.

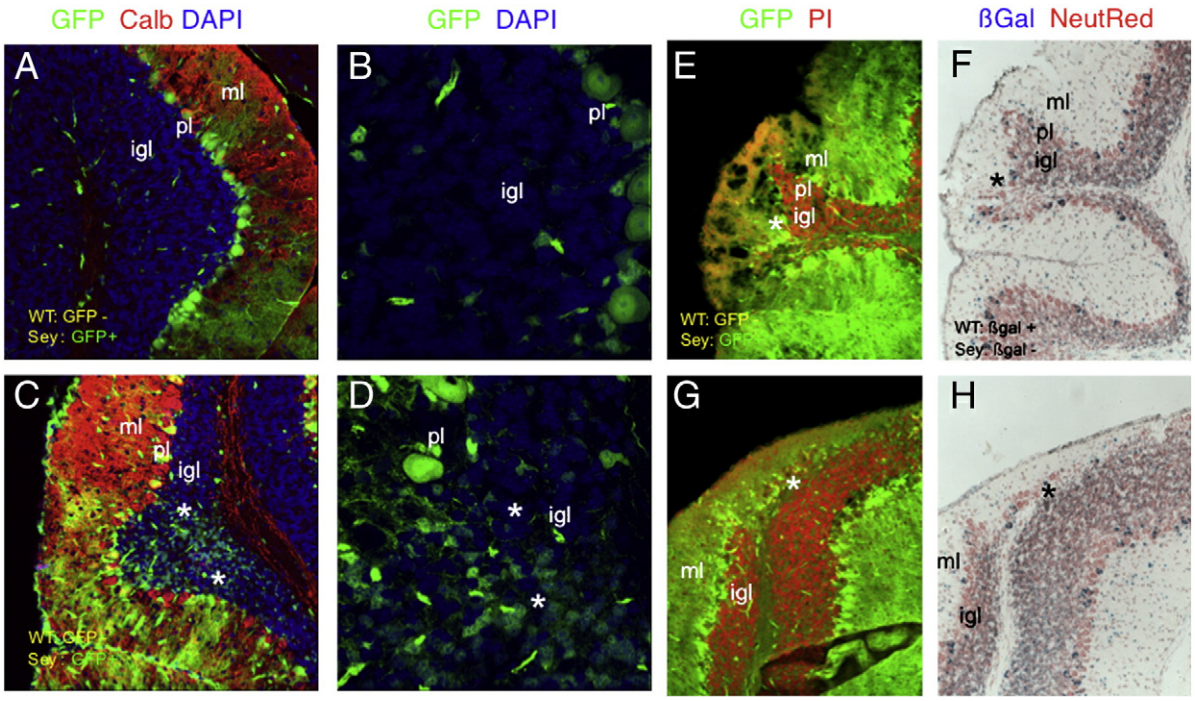

Fig. 2. (A–D) Mutant granule cell deficits in P21 chimeras. As indicated with β-Gal histochemistry in Fig. 1 Panel C, in the Pax6-null<->Rosa26 mutant chimera (X1291), Pax6-null granule cells are absent from the IGL in the anterior lobule 3, being predominated by GFP-negative granule cells (A, B detail), whereas GFP-positive mutant granule cells colonize the IGL in regions of the intermediate lobule (asterisks, C, D). A substantial cohort of normally placed Purkinje cells of mutant origin (Green/GFP and Red/Calb, calbindin) is found in the same region. Intermediate lobules of the lateral cerebellum show cellular disruptions consistent with loss of granule cells in the IGL (E, F, G, and H). There is a distinct absence of Pax6-null cells in these areas (asterisks). Propidium iodide (PI) in I and J and Neutral Red (NeutRed) in G and H were used as counterstains of cell bodies. Internal granule cell layer (igl), Pukinje cell layer (pl), molecular layer (ml).

(arrows in Fig. 1C, E, and asterisks in Fig. 2C, D). In the lateral cerebellum, this regional bias is still present with an increased number of Pax6-null granule cells (Fig. 1D, F). Laterally, in areas with an equal mixture of mutant and wildtype granule cells, there is a normal-appearing trilaminar organization of the cerebellum. However, in paravermal regions, the pockets of disrupted cytoarchitecture represent a loss of IGL cells and a disruption of the normal monolayer of Purkinje cells in this area (asterisks in Fig. 2E–H). Remnants of Pax6-null (GFP-positive) granule cells are seen in these pockets and are bounded by a normal IGL composed of exclusively wildtype granule cells. The small nests of subpial granule cells are strictly of the Pax6-null genotype (data not shown). The Purkinje cell population displays a consistent intermingling of cells of both genotypes throughout the entire cerebellum (Note mixed markers in the Purkinje cell layer (pl) in Fig. 2A–H). This normal distribution of mutant Purkinje cells is consistent for all ages examined, emphasizing the granule cell autonomous nature of the Pax6 mutation.

The intriguing bias in the colonization of the granule cell population in mutant chimeras raises several questions: does the regional absence of Pax6-null granule cells result from their inability to colonize the IGL or the subsequent elimination of cells that reach the IGL? Conversely, what are the antecedents of the overrepresentation of Pax6-null granule cells in other regions? To answer these questions, we examined younger chimeras to observe the developmental sequelae that led to the phenotypes defined in the mature chimeric cerebellum.

The P10 Pax6-null chimera cerebellar phenotype

The overall morphology of the P10.5 mutant chimeric cerebellum shows a range from small to normal, with the more affected chimeras (those with noticeably smaller cerebella) exhibiting a diminution of complexity in foliation, particularly in vermal lobules VI and VII (Fig. 3A–H). An obvious cytological abnormality in mutant chimeras is the presence of chains of radially oriented granule cells formed in the molecular layer of lobules VII-VIII in the medial and lateral cerebellum (Fig. 3I). Additionally, at paravermal levels, a population of granule cells can be found extending anteriorly beyond the normal cerebellar border into the adjacent midbrain tissue, reminiscent of the extracerebellar migration seen in homozygous mutant embryos (Fig. 3J) (Engelkamp et al., 1999; Swanson et al., 2005).

Of particular note, the regions of the P10 mutant chimeric cerebellum that demonstrate the greatest cytological disruptions are the same regions in the P21 chimeric cerebellum with abnormalities in granule and Purkinje cells. Some of the features observed in the P21 chimeras, e.g. the thinning of the IGL, near-total loss of granule cells, and the disruption of the Purkinje cell layer, are not obvious in the P10 chimeras, suggesting that these events occurred after P10 in the Sey chimeric cerebellum. An examination of cell genotype is critical to gain insights into the role that Pax6-null granule cells play in disrupted cerebellar morphogenesis.

Pax6-null cells in the P10 chimeric EGL

In contrast to the paucity of Pax6-null granule cells in the IGL of the P21 medial cerebellum, numerous mutant granule cell precursors colonize the cerebellar EGL in P10.5 chimeras throughout the anteroposterior extent of the cerebellum (Fig. 4). Mutant granule cell precursors are found in medial as well as lateral regions of the EGL, indicating that the tangential migration of EGL neuroblasts can occur throughout the full extent of the cerebellum (Fig. 4A, D). In contrast to wildtype chimeras, the EGL of the mutant chimera shows discrete patches of Pax6-null (GFP-positive) and wildtype (GFP-negative) cells with a graded mixing of the cells in transition from one large patch to the next (Fig. 4A, D). Where the EGL is largely colonized by Pax6-null granule cell progenitors, the few wildtype cells of the EGL are found almost entirely in the deepest aspects of the EGL and this is mirrored in the preferential colonization of the EGL by wildtype cells (see below). Finally, in the lateral cerebellum, the population of cells migrating beyond the cerebellar boundary is made up entirely of

mutant granule cells, indicating the granule cell autonomous nature of this mutant phenotype (Fig. 4F). This structure appears to form an extracerebellar mutant EGL similar to the extracerebellar migration observed in Pax6-null homozygous embryos (Engelkamp et al., 1999; Swanson et al., 2005) and in Unc5h3 mutant chimeras (Goldowitz et al., 2000).

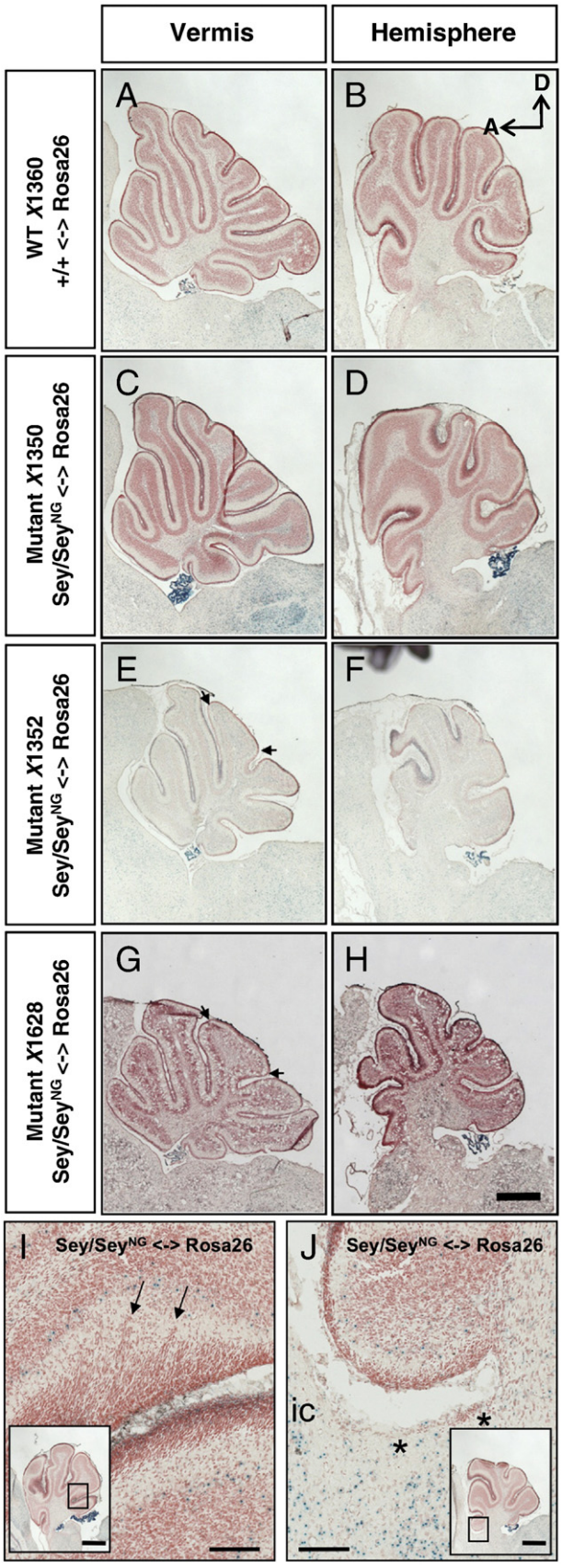

Pax6-null cells in the P10 chimeric IGL

The lack of colonization of the IGL by mutant cells stands in stark contrast to the more extensive colonization in EGL described above. In wildtype chimeras or mosaic cerebella, there is a generally one-to-one correspondence in the proportion of EGL cells to IGL cells with relation to the genotype in wildtype chimeras (Espinosa and Luo, 2008; Ryder and Cepko, 1994; Swanson and Goldowitz, unpublished results). This radial relationship between EGL and IGL, however, is not seen in P10 mutant chimeras. There are two distinct patterns of IGL colonization typical in mutant chimeras in regions where the EGL is predominantly mutant. First, the IGL of anterior and posterior lobules are nearly devoid of mutant granule cells even when the EGL is heavily populated with mutant granule cell precursors (Fig. 4A, B, D). Second, in contrast, the IGL of the central lobules shows a high level of colonization by mutant granule cells (Fig. 4A, C, D). Medially, this colonization is typically restricted to lobule VII and this territory of IGL colonization expands into adjacent lobules in the cerebellar hemispheres (Fig. 4A, C, D, E). These findings suggest there is a severe regional impairment in radial migration, survival, or a combination of the two.

Pax6-null cells in the P10 chimeric ML

By examining the genotype of migrating cells, we can determine the capacity of Pax6-null granule cells to migrate radially. In regions where the EGL is mainly composed of wildtype cells, the radially migrating, spindle-shaped cells in the ML are almost entirely genetically wildtype (Fig. 4A). Where there is high mutant EGL colonization migration of granule cells is seen in two different patterns. First, in anterior and posterior lobules where greater than 90% of the EGL cells are Pax6-null, mutant cells comprise fewer than 30% of the migrating cells in the ML and far fewer are found residing in the IGL (Fig. 4B). Second, in regions where Pax6-null granule cells colonize the IGL, a greater proportion of mutant cells migrate through the ML. Moreover, migration occurs in one of two modes. In lobules where there is mixing of wildtype and mutant cells in the IGL (e.g. in central lobule VIII), cells of both genotypes migrate in a relatively normal radial manner, although not in proportion to the relative contribution to the EGL and results in a wildtype bias in the IGL (Fig. 7F). In lobules with high mutant colonization of the IGL (e.g. medial and lateral central lobule VII), the vast majority of cells migrating through the ML are mutant (Fig. 4C, E). However, rather than well-spaced single cells and migrating chains, mutant cells are clumped in large clusters or “raphes” that span the ML.

The abnormality in migration raises the issue whether mutant glia might be at the root of these migratory defects. If this were the case, one would expect to see genetically normal glia relegated to regions where there was normal migration and Pax6-null glia in regions where there is aberrant migration. This, however, is not the case, for example, in the posterior lobule X where wildtype cells successfully migrate and mutant cells do not. Here, GFAP staining highlights a

Fig. 3. P10 mutant chimeras have small cerebella and regional foliation defects. (A–H) Medial vermis and lateral hemisphere sections of the cerebellum from a wildtype chimera (X1360, A, B) and Sey/Sey<->Rosa26 mutant chimeras (X1350; C, D, X1352 E,F and X1628 G, H) were stained for β-Gal activity and counterstained with neutral red. The mutant chimeric cerebella are smaller than the wildtype cerebella and are underfoliated in the central lobules (small arrows in E and G designate the superficial boundaries of the affected lobules V-VII in these chimeras). (I) Abnormal cellular raphes (arrows) streaming through the molecular layer are common in Pax6-null chimeras. (J) An ectopic cohort of granule cells (asterisks) extends beyond the cerebellar boundary into the inferior colliculus (ic). Orientation arrows point dorsal (D) and anterior (A).

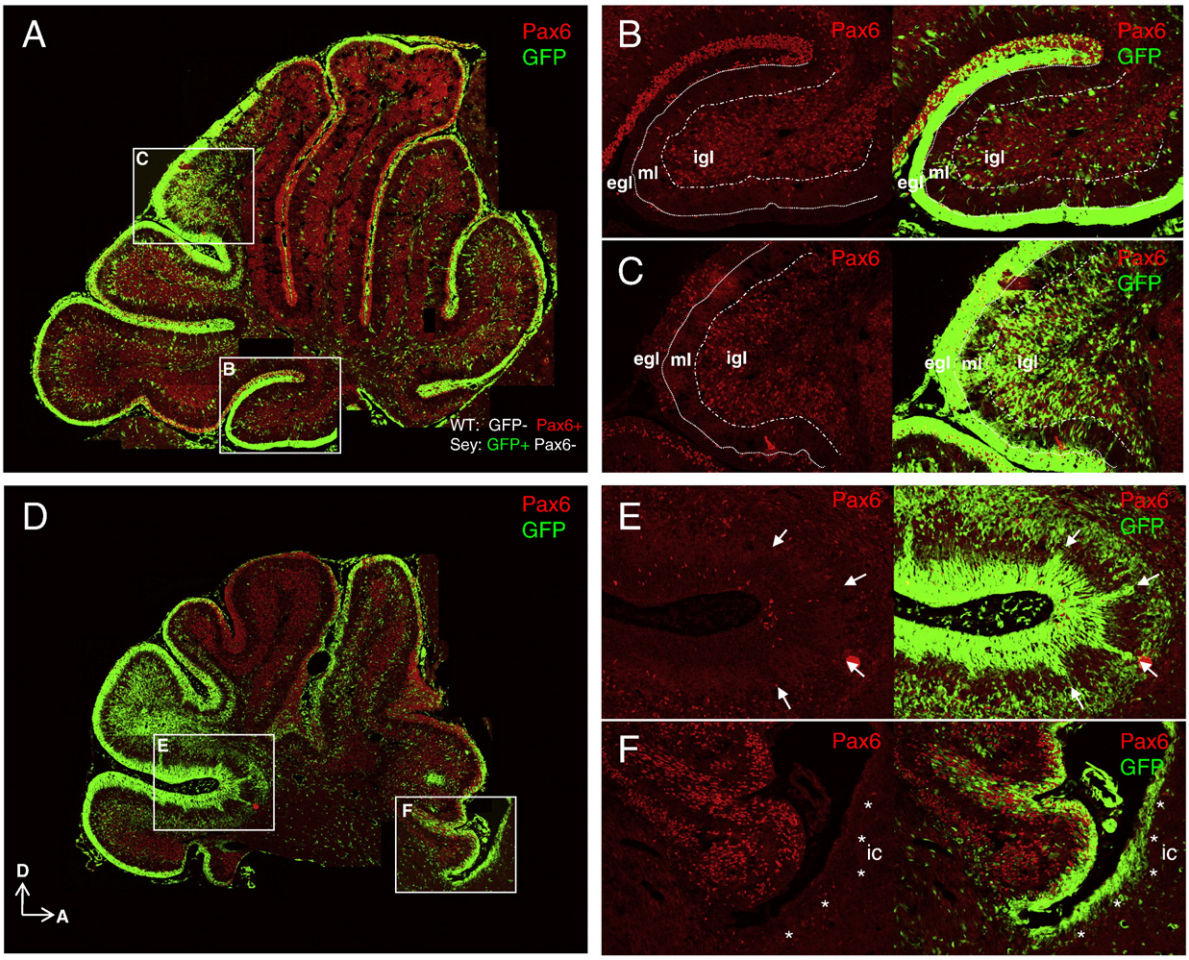

Fig. 4. Colonization of IGL by Pax6-null granule cells is regionally dependent. (A, D) Confocal photomontages of a P10 Sey/Sey<->BalbC chimera (X1741) from the midline vermis (A) and lateral hemisphere (D) showing native GFP fluorescence (green) and Pax6 immunofluorescence (red). Pax6-null granule cells are Pax6-negative and GFP-positive, and wildtype host cells are Pax6-positive and GFP-negative. (B) Posterior lobule X shows a high percentage mutant EGL with few GFP-positive cells migrating into the IGL, which is dominated by wildtype cells. (C) Intermediate lobule VII shows a high percentage mutant EGL and an abundance of mutant cells mixed with wildtype cells in the IGL. (E) Granule cell raphes (arrows) penetrating through the molecular layer in the lateral cerebellum are almost entirely Pax6-negative and GFP-positive mutant granule cells. (F) In the anterior lateral hemisphere an ectopic EGL-like structure (asterisks) extends into the inferior colliculus (ic) and is exclusively of mutant origin (Pax6-negative and GFP-positive). Internal granule cell layer (igl), external granule cell layer (egl), molecular layer (ml). Orientation arrows point dorsal (D) and anterior (A).

normal complement of radially oriented glial processes, some of which are of mutant origin (Fig. 5A–B). Conversely, in a region where there is aberrant migration we find abnormal glial profiles, some of which belong to genetically wildtype glia (Fig. 5C–D). Importantly, in regions with predominantly wildtype granule cell migration, Bergmann glial fibers of mutant origin appear to have a normal morphology and are seen to support normal migration of wildtype cells from the EGL (Fig. 5E–H). Thus, it seems likely that the migration deficit observed in mutant granule cells is intrinsic to this cell population and not related to genetically mutant glia.

Incomplete differentiation of Pax6-null granule cells

The finding of absent or aberrant migration of mutant granule cells in the face of normal glia, and vice versa, suggests that the developmental program of the Pax6-null granule cell is abnormal. βIII-tubulin (TuJ1) was used to explore the differentiation status of Pax6-null granule cells in the EGL. Normally, as granule cell precursors exit the cell cycle and move to the inner EGL, they begin to express the TuJ1 marker. Thus, in the P10 Pax6-null chimeric cerebellum wildtype granule cells display the typical TuJ1-positive profile restricted to the inner EGL (egl^i in Fig. 6A, B). A dense TuJ1-positive inner EGL and a strong signal in the ML, likely reflecting expression of TuJ1 in the parallel fiber processes, is also seen in regions with an abundance of mutant EGL and IGL granule cells (Fig. 6C, D). This contrasts with the TuJ1-negative outer EGL (egl^o in Fig. 6) where the typically immature granule cell precursors reside. In the regions of minimal mutant cell migration, the TuJ1 expression of the mutant EGL cells is compressed into a thinner inner EGL area, suggesting that fewer cells make up this zone of differentiation (egl^i in Fig. 6E, F).

We also examined Ki67 in order to assess the proliferative status of the Pax6-null granule cells. In wild type cells, Ki67 expression is localized to the proliferative cells of the outer EGL and is in contrast to the Ki67-negative, postmitotic, inner EGL cells (egl^o and egl^i respectively in Fig. 7A–C). In regions with high percentages of Pax6-null EGL cells, Ki67 expression extends through the entire width of the EGL, displaying no clear distinction of the inner or outer EGL with this marker ($egl^{o/i}$ in Fig. 7D–F). Strikingly, the mutant granule cells seen migrating in the cellular raphes in these regions also express Ki67 at the same intensity as seen in the cells of the EGL (arrows in Fig. 7G–I), suggesting that these cells have not exited the cell cycle even as they are exhibiting behaviors of a differentiating granule cell.

Morphological defects in the neonatal Pax6-null chimeric cerebellum

In the P0.5–1.5 normal and control chimeras, the cerebellum is beginning to transform from a uniform surface into a foliated structure with the appearance of the primary fissure, separating the

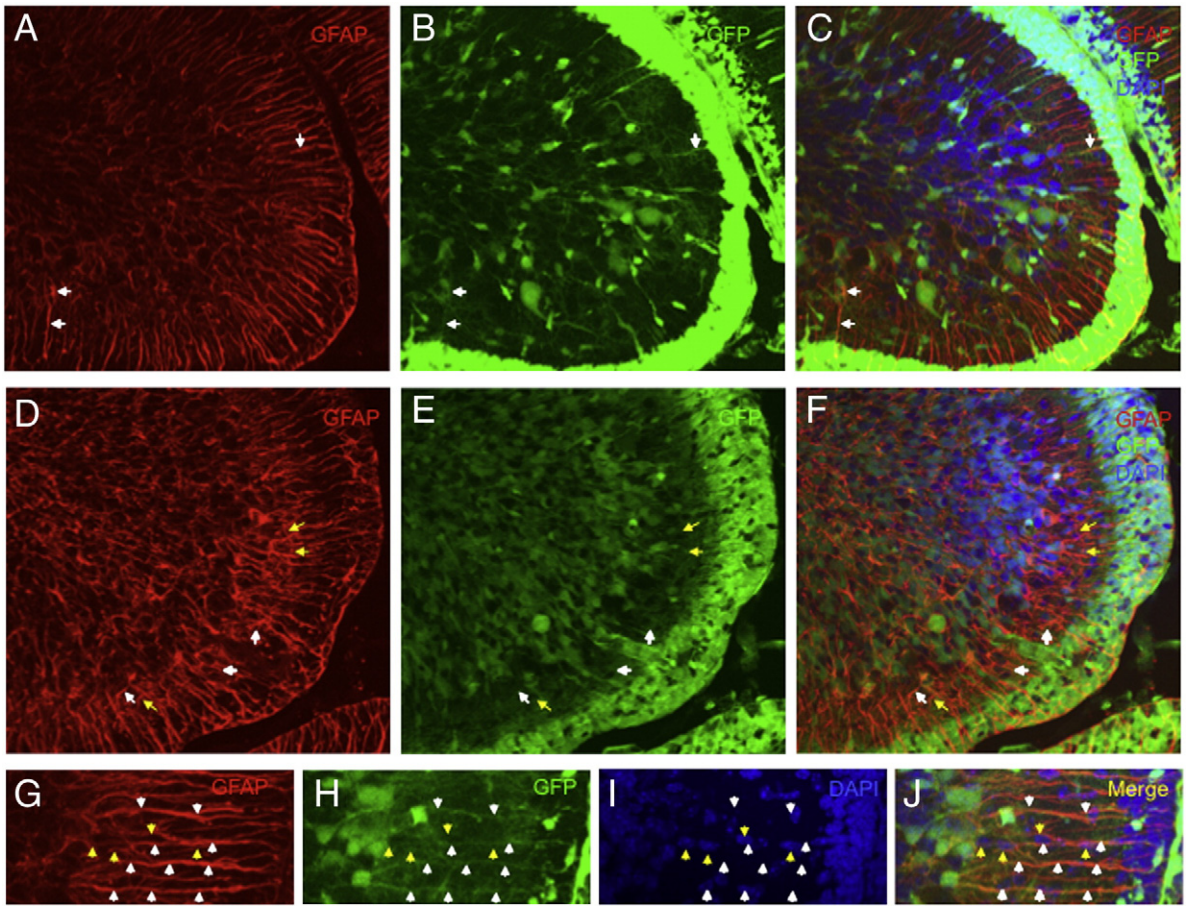

Fig. 5. Pax6-null radial glial cells and fibers can support cell migration. A P10 mutant chimera (X1741) was labeled with anti-GFAP (red) to label glial processes, GFP fluorescence (green) to label all Pax6-null cells (neurons and glia), and counterstained with DAPI (blue) to label all nuclei. (A-C) GFAP-positive Bergmann glial processes appear normal in the posterior lobule X, where Pax6-null granule cell migration is deficient. White arrowheads highlight Pax6-null radial glial cells (GFP-positive) and their normal-appearing Bergmann glial processes (co-stained for GFAP). (D–F) In another section from the same chimera, in lobule VII where there is a high percentage of Pax6-null granule cells, the molecular layer is populated by many histologically abnormal radial glial processes, some of Pax6 mutant origin (GFP-positive, white arrowheads) and others of wildtype origin (GFP-negative, yellow arrows). (G–J) Pax6 mutant radial glial fibers (GFAP-positive and GFP-positive; white arrowheads) have a normal appearance and support migration of wildtype granule cells through the molecular layer (DAPI + nuclei; yellow arrowheads).

anterior and posterior aspects of the cerebellum. In this respect, a range of phenotypes is seen in our neonatal mutant chimeras. At the high range of mutant percent chimerism (i.e. 80–99% mutant), chimeras display a smaller, developmentally retarded cerebellum with either rudimentary fissures or with a mostly unfoliated cerebellum resembling the homozygous mutant neonatal cerebellum (Swanson et al., 2005; Engelkamp et al., 1999), which is most pronounced at midline (Fig. 8F–G). Mid-range chimeras (approximately 40–70% genotypically mutant) display an unusual combination of normal and abnormal cerebellar morphologies admixed within the cerebellum. In some of these mice the medial cerebellum shows relatively normal foliation. Other individuals have typical anterior lobules with clear preculminate and primary fissures, however, the posterior cerebellum is remarkably unfoliated with only rudimentary secondary and/or posterolateral fissure formation (Fig. 8C–E).

Cellular defects in the P0.5–1.5 Sey/Sey^{Neu} Chimera

In contrast to control chimeras, large portions of the EGL in mutant chimeras are primarily represented by one genotype or the other (Fig. 8A, C, F). We used a Math1:LacZ knockin allele (Ben-Arie et al., 1997) bred into the Sey mutant mouse strain as the source for Pax6-null cells in chimeras in order to allow discrete identification of mutant granule cell precursors in the developing EGL of chimeras while cells from the wildtype strain carrying a ubiquitously expressed GFP marker labeled all wildtype cells. In the medial cerebellum, wildtype cells dominate the EGL anteriorly and Pax6-null cells dominate the posterior EGL. Furthermore, the EGL in the hemispheres is composed almost entirely of mutant cells in moderate to high percentage chimeras (data not shown). This distinct segregation of genotypes most strikingly highlights the foliation defects seen in the mutant chimeras. Specifically, large patches of wildtype cells are found in the antero-medial chimeric cerebellum, where foliation patterning is the most normal, whereas, there is a loss of normal foliation wherever large patches of Pax6-null cells are found (e.g. postero-medial cerebellum; Fig. 8). Most intriguing is the observation that in chimeras where a rudimentary primary fissure has formed, there is a small aggregate of wildtype cells invariably associated with this fissure that is surrounded by mutant cells (Fig. 8). Often this wildtype cluster of cells is found at the deepest aspect of the nascent fissure and successful foliation appears linearly correlated with the number of wildtype granule cell precursors. Thus, mutant cells are unable to participate in the process of initiating a fissure.

One final point that is clear in the neonatal chimeras is that there is a widespread rescue of Purkinje cell migration. In the Pax6 mutant cerebellum about 30% of all Purkinje cells are ectopically located in the deep aspects of the corpus cerebelli (Swanson et al., 2005). In neonatal chimeras, virtually no Purkinje cells are found in this ectopic location. This is the case even in high percentage mutant chimeras. Similar results have been reported in reeler chimeras where a limited number of wildtype granule cells can largely rescue Purkinje cell ectopia (Mullen et al., 1997). This also emphasizes the non-cell

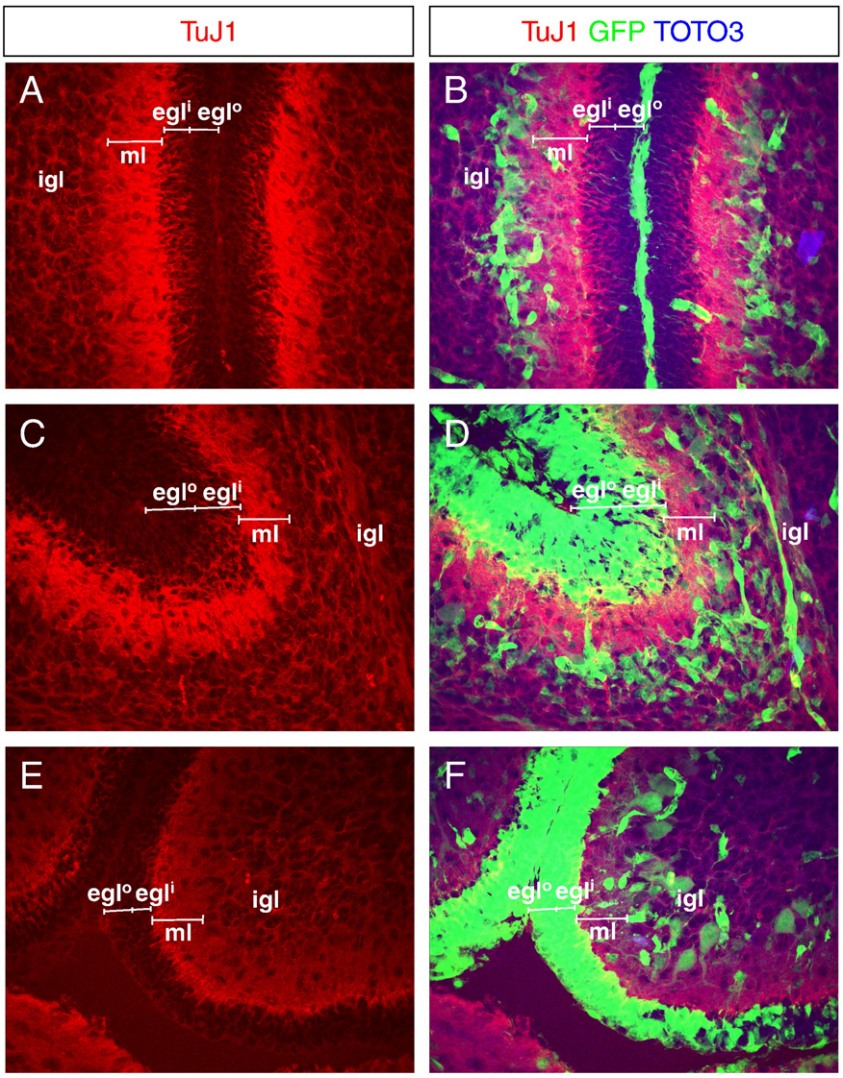

Fig. 6. TuJ1 expression pattern in mutant chimeras. (A, B) Wildtype cells (GFP-negative) in this mutant chimera (X1352) display a normal TuJ1 expression in cells of the inner EGL (egl^i) and is strong in the molecular layer (ml), likely reflecting expression in the parallel fibers but is absent from the proliferative outer EGL (egl^o). (C, D) In the central lobules, a region with a high proportion of mutant cells and extensive migration into the IGL, the TuJ1 expression pattern is also normal restricted to the inner EGL and the molecular layer. (E, F) In the posterior lobule with unsuccessful mutant cell migration TuJ1-immunoreactivity is dramatically limited, relegated to a thin layer in the inner EGL and diminished in the ML. Note that in all cases the laminar pattern of TuJ1 expression in relatively normal and not distributed throughout the EGL.

autonomous nature of the Purkinje cell ectopic phenotype in the homozygous Pax6 mutant cerebellum.

Discussion

Using experimental mouse chimeras, we are able to follow postnatal development of Pax6-null cerebellar cells and surmise their potential well beyond the timeframe of the neonatal lethality inherent with the homozygous Sey mutant. We have shown a largely cell-autonomous failure of Pax6-null granule cells to fully integrate into the mature cerebellum. It is presumed that the reduced developmental capacity of the Pax6-null granule cells results in the inability of these cells to read cues critical for initiation of fissurization as well as deficits in the normal expansion and migration of the postmitotic granule cell population, leading to a smaller cerebellum with underdeveloped foliation. Pax6-null cells are largely incapable of normal migration into the IGL. Furthermore, as these cells migrate they appear to retain characteristics of granule cell precursors, while showing features of mature neurons. Pax6 is necessary for critical aspects of intrinsic granule cell developmental programs as well as granule cell interactions with the cerebellar environment as they transition through these programs. While our data show that the influence of the Pax6 mutation is largely cell autonomous with respect to the cerebellar granule cell, the influence of this mutation on cerebellar development through subtle influences on other cell types cannot be entirely excluded.

Failure of Pax6-null cells to participate in foliation

pt?>The defects in foliation seen in Pax6-null chimeras are informative to the normal mechanisms underlying fissure formation. Limited fissure formation is seen in the neonatal mutant chimera when Pax6-null EGL cells dominate the anterior cerebellum. When there is successful fissure initiation we invariably find a preponderance of wildtype EGL cells at the base of the forming fissure. Sudarov and Joyner (2007) described the first signs of these foliation anchor centers as fulcrums where EGL cells have distinct shape changes and an increased mitotic index. They determined that granule cell precursors were the primary drivers of the location and timing of fissure formation. The actual substrate that dictates the precise location and timing of anchor point initiation is still unclear. Engelkamp and colleagues (1999) showed that while overt foliation was absent in the embryonic Pax6-null cerebellum, several cellular markers (including PSA-NCAM and Pax2-positive cellular migration) delineated a Pax6-independent folial organization in the

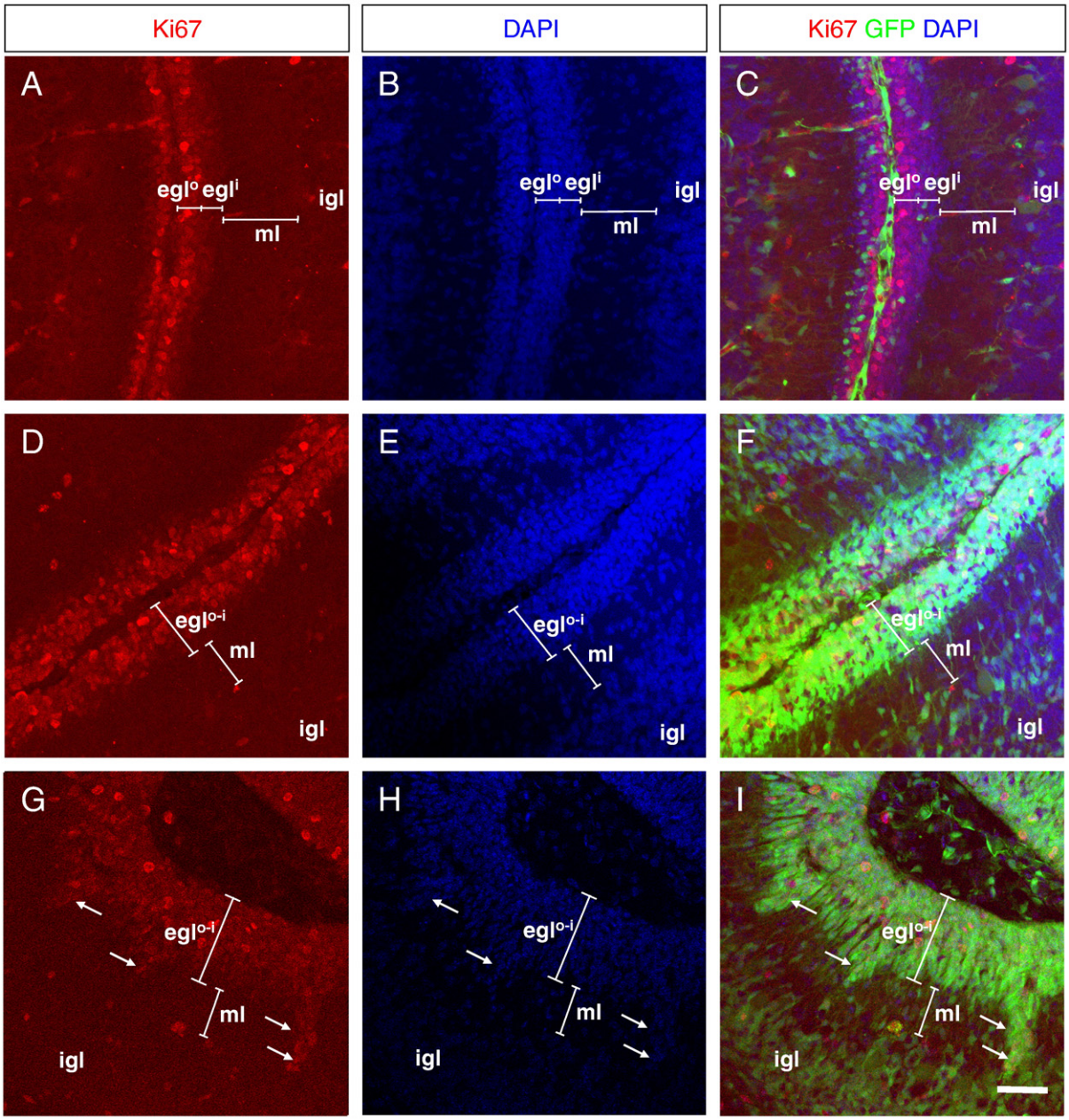

Fig. 7. Pax6-null granule cells retain immature Ki67 phenotype. (A–C) In a wild-type region of a P10 chimeric cerebellum (X1741), The expression of Ki67 (red) is detectable but at low levels in all cells restricted to the outer EGL (egl^o), with an occasional intensely labeled cell (presumably S-phase), reflecting the actively proliferating progenitor population of the EGL. (D–F) Ki67 expression is seen throughout the EGL where the EGL is composed almost entirely of GFP-positive (green) Pax6-null cells. Here, there is no distinction between inner and outer EGL zones of Ki67 immunoreactive cells ($egl^{o/i}$. (G–I) The cellular streams of radially migrating mutant cells (arrows) are also positive for Ki67 immunoreactivity with intensely labeled cells seen deep in the ML quite uncharacteristic of normal migrating cells.

underlying cerebellum. Our present findings confirm that wildtype granule cells are critical for this process and that Pax6-null cells cannot participate in this key developmental event. Even when there are very few wildtype cells, they preferentially congregate at the appropriate points of foliation, suggesting an active recognition of the signal(s) that determine the anchor point locations. Thus, Pax6 expression is required for granule cell precursors to either read or respond to an as-yet-identified signal (as suggested in Sudarov and Joyner, 2007) that triggers the granule cell program that initiates fissure formation.

Smaller cerebellum and regulation of granule cell number

One of the most overt phenotypes found in the Pax6-null chimera is the reduced size and underdeveloped nature of the cerebellum. The greater the contribution of the Pax6-null granule cell precursors the more severe this effect. Whereas, postnatal growth of the cerebellum is considered to be the consequence of the explosion of granule cell neurogenesis, our results place Pax6 in a critical position in the developmental programs necessary for granule cell genesis and cerebellar growth. Genetic or environmental insults that affect the granule cell population size have a strict temporal dependency under which the population can either recover or succumb. If a mitotic poison (e.g., FUdR or MAM) or X-irradiation targets cells during the main period of granule cell neurogenesis, the granule cell progenitors are capable of compensation to produce a near-normal number of granule cells (Altman et al., 1969; Shimada and Langman, 1970). In the meander tail mouse cerebellum there is a near-total loss of anterior lobe granule cells during the expansion phase of this population. However, in meander tail chimeras, with as few as 40% wildtype cells, the wildtype cerebellar granule cell population

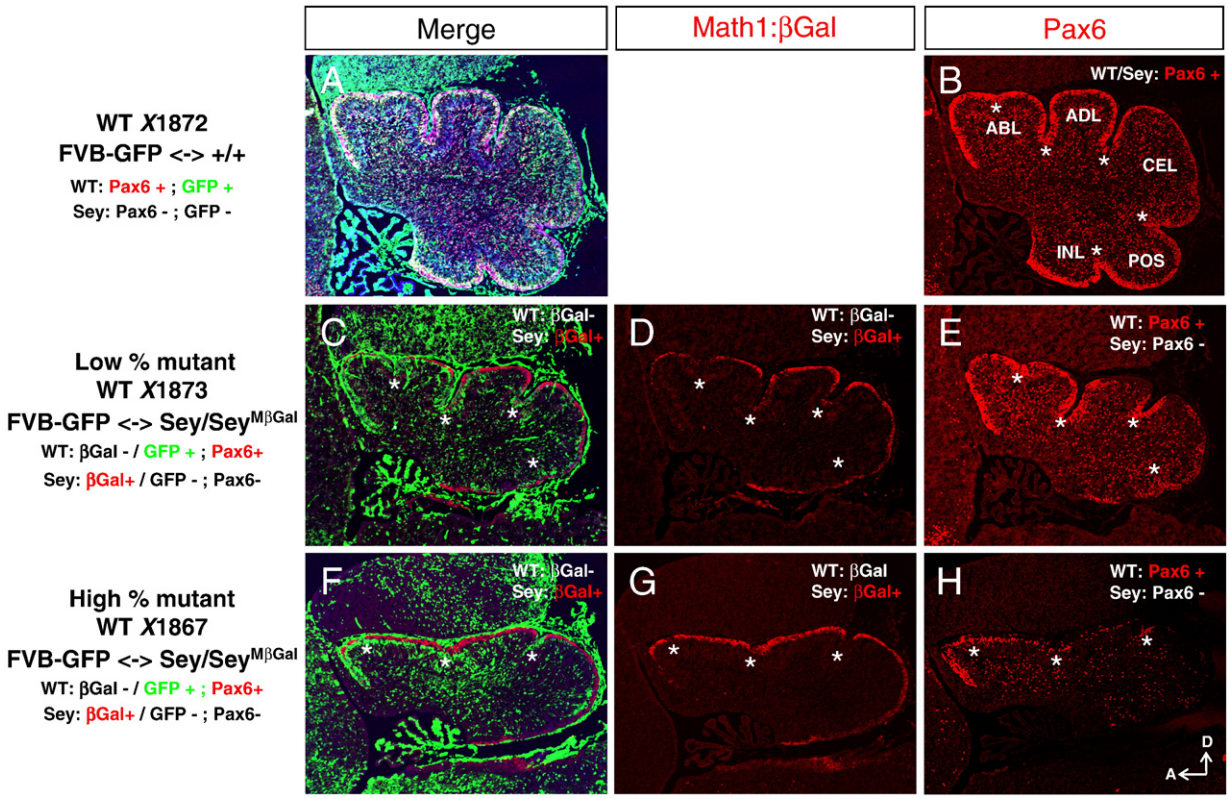

Fig. 8. Segregation of EGL cells by genotype emphasizes wildtype cell determination of anchor points for initial foliation in neonatal mutant chimeras. (A, B) P1.5 wildtype chimera is double-labeled for Pax6-positive granule cells (red) and GFP fluorescence (green, merged) to illustrate the broad mixing of granule cells throughout this chimeric cerebellum and show the normal cardinal lobe formation separated by four well defined fissures (asterisks), anterior basal lobe (ABL), anterior dorsal lobe (ADL), central lobe (CEL), posterior lobe (POS), and inferior lobe (INL). (C–H) Two neonatal mutant chimeras carrying the Math1:LacZ allele in cells from the Sey strain and a ubiquitously expressed GFP allele in cells from the wildtype strain (C–E, P1.5; F–H, P0.5). In these chimeras, β-Gal (red, C, D and F, G) specifically identifies the mutant granule cell precursors and all wildtype cells are GFP-positive (green). (C, F) Double labeling of sections for β-Gal immunoreactivity and GFP fluorescence highlights the discrete patches of complimentary populations of mutant and wildtype cells in the EGL. (D, G) Mutant EGL cells visualized with β-Gal immunostaining illustrating their absence from the depths of each fissure (asterisks). (E, H) Pax6 (red) immunostaining in adjacent sections demonstrates the presence of wildtype cells at these points of fissurization (asterisks). Orientation arrows point dorsal (D) and anterior (A). Note that the distinction of the posterior and inferior lobules is obscured in the mutant chimeras, and these are regions where there are few wildtype EGL cells.

overcomes the deletion of mutant cells and restores the anterior lobe to normal size (Hamre and Goldowitz, 1997). This is in distinction to defects in granule cell development that precede or follow EGL mitotic activity. A defect that precedes EGL formation is illustrated in Math1-null chimeras, where the mutant cohort of progenitor cells in the rhombic lip is deleted early, resulting in a cerebellum with substantially fewer granule cells (Jensen et al., 2004). Defects following EGL proliferation are seen in the weaver mutant where granule cells die in the migratory phase of development (Rakic and Sidman, 1973) and in the weaver chimeric cerebellum there is no rescue of cell number by wildtype cells (Goldowitz, 1989). Thus, the inability of wildtype cells to restore granule cell numbers in the Pax6-null chimeric situation provides evidence that an event in the early postmitotic life of the granule cell is disrupted by the Pax6 mutation.

Uncoordinated neuronal differentiation in Pax6-null granule cells

One striking finding regarding the differentiation state of the Pax6-null granule cells is that they express characteristics of both proliferating and differentiating cells. They appear to initiate a normal differentiation program by expressing neuronal βIII-tubulin appropriately, while retaining the low level Ki67 expression characteristic of mitotically active progenitor cells. Furthermore, we observed mitotically active Pax6-null cells in radially migrating streams, which is never seen in migrating wildtype cells. Thus, it appears that the differentiation of these cells is incomplete, retaining an immature character while undergoing behaviors relegated to more mature differentiated granule cells. Interestingly, a similar phenotype has been observed in a Math1 overexpressing mouse (Helms et al., 2001), in which EGL cells displayed overlapping differentiation and proliferation markers, and Pax6 expression was also drastically reduced providing an explanation for the cellular phenotype. Our in vivo results are reminiscent of findings in cultured Sey/Sey granule cells, expressing markers for active proliferation even as these cells expressed markers of neuronal differentiation (Swanson et al., 2005). Yang et al. (2003, 2006) have suggested that re-entry of differentiated neurons into the mitotic cycle facilitates degeneration of these cells in Alzheimer's disease. Thus, the reduced presence of mutant cells in the anterior and posterior lobules and the discernable architectural disruptions in the intermediate lobules may be due to the subsequent degeneration of the remaining mutant granule cells.

Tangential migration deficits in Pax6-null granule cell progenitors

Pax6-null granule cells in the mature postnatal cerebellum are absent from the anterior and posterior lobules of the vermis and have a limited colonization of the IGL of the central lobules. How this restricted colonization is realized in mutant chimeras highlights the roles that Pax6 plays in the local and global organization of the EGL that is established via tangential migration.

Pax6-null granule cell progenitors are present in segregated clusters or patches in the EGL of mutant chimeras that is in contrast to the extensive mixing of EGL cells in wildtype chimeras. This atypical segregation was seen at the earliest ages examined and suggests that as EGL cells exit from the rhombic lip to migrate on the

cerebellar surface, they maintain their distinct wildtype and mutant identities. This finding is consistent with the notion of a predetermined address for cohorts of granule cell progenitors which has been suggested in Math1 mutant chimeras, where physical gaps in the EGL were seen where the Math1-null cells failed to exit the rhombic lip (Jensen et al., 2004). A similar level of segregation of Pax6-null cells was observed in the developing cerebral cortex and eye in chimeras and in vitro models, and it has been suggested that Pax6 is critical for controlling cell surface properties that support cellular interactions and migration (Collinson et al., 2000; Stoykova et al., 1997; Talamillo et al., 2003). The suggested roles for Pax6 in regulating L1cam, Ncam and R-cadherin gene expression in neurons (Andrews and Mastick, 2003; Berger et al., 2007; Meech et al., 1999; Stoykova et al., 1997) are obvious modes by which Pax6 may regulate cell surface properties and cell–cell interactions in granule cell precursors. Thus, wildtype granule cells with normal homotypic cell surface interactions leave the rhombic lip and are free to intermingle within the developing EGL. Whereas Pax6-null granule cell progenitors exit from the rhombic lip and maintain their strict "address" in the EGL due to their altered cell surface and cell–cell adhesion properties. This would have profound influences as the cerebellum develops relative to their interactions with the environment in relation to foliation, tangential migration, proliferative expansion, and radial migration.

At the global level of EGL organization in the mutant chimera there is a posterior-lateral bias of mutant cells resulting in the marked reduction in the proportion of anterior-medial mutant cells. The anterior compartment of granule cell progenitors is the earliest generated population and the others are subsequent to this with the central lobules developing last (Hawkes et al., 1999; Machold and Fishell, 2005; Sgaier et al., 2005). An intrinsic developmental delay has been postulated to explain the cerebellar phenotype in the neonatal homozygous mutant (Engelkamp et al., 1999; Swanson et al., 2005). Such a delay intrinsic to the Pax6-null granule cell progenitors (GCPs) would put these cells at a distinct disadvantage for contributing to the early developing antero-medial compartment. This would lead to a reduced representation of Pax6-null cells in the anterior EGL of neonatal chimeras as they are out-competed by wildtype cells in the course of their anterior migration. Interestingly, the mutant population of GCPs is not diminished resulting in an over-representation of mutant GCPs in the later developing central/posterior compartments.

Deficits in radial migration of Pax6-null granule cells

One of the most striking phenotypes in the Pax6-null chimera is the large scale failure of mutant granule cells to migrate into the IGL. This is seen most vividly in P10 chimeras where there is an increasing proportion of the EGL shifted toward a Pax6-null cell bias across much of the cerebellum. This bias is most likely due to the successful migration of wildtype cells into the IGL leaving behind the non-migrating Pax6-null cells. These cells never successfully colonize the IGL as seen in the mature chimeric cerebellum. This migration defect is consistent with a previous report where granule cells remain in the EGL following retroviral transduction of a dominant negative Pax6 isoform (Yamasaki et al., 2001). We have also shown that the radial glial substrates in these lobules are normal and support wildtype cell migration. Thus, this migration defect in the Pax6-null cells must be intrinsic to the granule cells themselves. This cell intrinsic failure to undergo radial migration is also apparent in the population of mutant cells that aberrantly extend into the inferior colliculus, where they form an exclusively mutant extracellular EGL, but do not migrate internally to form an ectopic IGL (as they do in Unc5h3 mutant chimeras; Goldowitz et al., 2000). While the extracerebellar tangential migration is suggested to be related to a decreased Unc5h3 expression in the Pax6-null granule cells (Engelkamp et al., 1999), the deficit in radial migration must be due to other influences of the Pax6 loss of function.

In the central lobules, Pax6-null cells are observed to cross the ML abnormally. In this region, where there are fewer wildtype cells, the Pax6-null cells emerge from the EGL in large raphes. A more subdued form of this migration has been described in the wildtype chick and mouse cerebellum (Karam et al, 2001; Lin and Cepko, 1998). These normal raphes occur only during the early postnatal period and are distributed throughout the cerebellum. Although they resemble the early structures, the mutant raphes in the Pax6-null cerebellum are the primary mode of migration and only occur in the central lobules when there is an abundance of mutant EGL granule cells. However, it is unclear whether these unusual raphes are an accentuation of what is otherwise a normal (albeit developmentally early) mode of migration or a novel aberrant phenotype.

A minor population of mutant granule cells appears to follow the more traditional single-file and radial path to the IGL. These cells are found in the transitions between anterior and central lobules as well as in transitions between central and posterior lobules where there is often a high percentage of wildtype cells mixed with a limited number of mutant cells in the EGL. There are two possibilities to explain why some mutant granule cells are capable of normal migration. One hypothesis is that wildtype cells, which are in vast majority, may be providing instructional cues to Pax6-null granule cells in this region, akin to the findings of a community effect in the scrambler mutant (Yang et al., 2002). An explanation that resonates better with the theme that is emerging across Pax6-null phenotypes is that successfully migrating cells occur at a watershed of developmental time, in between early and late developing compartments that have either totally aborted migration (early) or migrated in an aberrant fashion (late). Thus, in regions of absent migration, a delayed competence of granule cell migration may result in missing a window of opportunity for responding to migration cues. While in the central lobules (which are later developing regions), the support of migrating wildtype cells is absent, the Pax6-null granule cells respond via a developmentally earlier migration mode taking the form of the cellular raphes.

In either case our results demonstrate the critical nature of Pax6 in radial migration of cerebellar granule cells.

Conclusion

In using experimental mouse chimeras we have illuminated distinct postnatal phenotypes of the Pax6-null granule cell that have previously been refractory to study. Our results indicate that Pax6 is critical for coordinating the developmental programs necessary for the cerebellar granule cell to complete its developmental journey and appears to have a critical function during the transition from a committed progenitor cell to a fully mature cerebellar granule neuron. Our findings offer the hypothesis that converges on the inability of Pax6 mutant cells to read cell/environmental signals during their developmental history. Thus, whether the signal is to position themselves to drive foliation, differentiation, or migration, the Pax6-null granule cell is severely impaired leading to their failure to participate in cerebellar development.

Acknowledgments

We thank Richard Cushing, Meifen Lu, Erich Brauer, Nobel Del Mar, and Drew Jervis for their expert technical assistance. We thank Drs. Matt Larouche and Thomas Ha for their critical reading in preparation of this manuscript. Rob Grainger, Marilyn Fisher, Brigid Hogan, Andras Nagy, and Huda Zoghbi kindly provided primary stocks of mice used in these studies. This research was supported by NIH grant R01 HD52472 (DG).

References

Altman, J., Anderson, W.J., Wright, K.A., 1969. Early effects of x-irradiation of the cerebellum in infant rats: decimation and reconstitution of the external granular layer. Exp. Neurol. 24, 196–216.

Andrews, G.L., Mastick, G.S., 2003. R-cadherin is a Pax6-regulated, growth-promoting cue for pioneer axons. J. Neurosci. 23, 9873–9880.

Ben-Arie, N., Bellen, H.J., Armstrong, D.L., McCall, A.E., Gordadze, P.R., Guo, Q., Matzuk, M.M., Zoghbi, H.Y., 1997. Math1 is essential for genesis of cerebellar granule neurons. Nature 390, 169–172.

Berger, J., Berger, S., Tuoc, T.C., D'Amelio, M., Cecconi, F., Gorski, J.A., Jones, K.R., Gruss, P., Stoykova, A., 2007. Conditional activation of Pax6 in the developing cortex of transgenic mice causes progenitor apoptosis. Development 134, 1311–1322.

Bermingham, N.A., Hassan, B.A., Price, S.D., Vollrath, M.A., Ben-Arie, N., Eatock, R.A., Bellen, H.J., Lysakowski, A., Zoghbi, H.Y., 1999. Math1: an essential gene for the generation of inner ear hair cells. Science 284, 1837–1841.

Collinson, J.M., Hill, R.E., West, J.D., 2000. Different roles for Pax6 in the optic vesicle and facial epithelium mediate early morphogenesis of the murine eye. Development 127, 945–956.

Engelkamp, D., Rashbass, P., Seawright, A., van Heyningen, V., 1999. Role of Pax6 in development of the cerebellar system. Development 126, 3585–3596.

Ericson, J., Rashbass, P., Schedl, A., Brenner-Morton, S., Kawakami, A., van Heyningen, V., Jessell, T.M., Briscoe, J., 1997. Pax6 controls progenitor cell identity and neuronal fate in response to graded Shh signaling. Cell 90, 169–180.

Espinosa, J.S., Luo, L., 2008. Timing neurogenesis and differentiation: insights from quantitative clonal analyses of cerebellar granule cells. J. Neurosci. 28, 2301–2312.

Fink, A.J., Englund, C., Daza, R.A., Pham, D., Lau, C., Nivison, M., Kowalczyk, T., Hevner, R. F., 2006. Development of the deep cerebellar nuclei: transcription factors and cell migration from the rhombic lip. J. Neurosci. 26, 3066–3076.

Friedrich, G., Soriano, P., 1991. Promoter traps in embryonic stem cells: a genetic screen to identify and mutate developmental genes in mice. Genes Dev. 5, 1513–1523.

Grindley, J.C., Davidson, D.R., Hill, R.E., 1995. The role of Pax-6 in eye and nasal development. Development 121, 1433–1442.

Grindley, J.C., Hargett, L.K., Hill, R.E., Ross, A., Hogan, B.L., 1997. Disruption of PAX6 function in mice homozygous for the Pax6Sey-1Neu mutation produces abnormalities in the early development and regionalization of the diencephalons. Mech. Dev. 64, 111–126.

Goldowitz, D., 1989. The weaver granuloprival phenotype is due to intrinsic action of the mutant locus in granule cells: evidence from homozygous weaver chimeras. Neuron 2, 1565–1575.

Goldowitz, D., Mullen, R.J., 1982. Granule cell as a site of gene action in the weaver mouse cerebellum: evidence from heterozygous mutant chimeras. J. Neurosci. 2, 1474–1485.

Goldowitz, D., Hamre, K.M., Przyborski, S.A., Ackerman, S.L., 2000. Granule cells and cerebellar boundaries: analysis of Unc5h3 mutant chimeras. J. Neurosci. 20, 4129–4137.

Hadjantonakis, A.K., Macmaster, S., Nagy, A., 2002. Embryonic stem cells and mice expressing different GFP variants for multiple non-invasive reporter usage within a single animal. BMC Biotechnol. 2, 11.

Hamre, K.M., Goldowitz, D., 1997. meander tail acts intrinsic to granule cell precursors to disrupt cerebellar development: analysis of meander tail chimeric mice. Development 124, 4201-4012.

Hawkes, R., Beierbach, E., Tan, S.S., 1999. Granule cell dispersion is restricted across transverse boundaries in mouse chimeras. Eur. J. Neurosci. 11, 3800-3008.

Helms, A.W., Gowan, K., Abney, A., Savage, T., Johnson, J.E., 2001. Overexpression of MATH1 disrupts the coordination of neural differentiation in cerebellum development. Mol. Cell. Neurosci. 17, 671–682.

Hill, R.E., Favor, J., Hogan, B.L., Ton, C.C., Saunders, G.F., Hanson, I.M., Prosser, J., Jordan, T., Hastie, N.D., van Heyningen, V., 1991. Mouse small eye results from mutations in a paired-like homeobox-containing gene. Nature 354, 522–525.

Hogan, B.L., Horsburgh, G., Cohen, J., Hetherington, C.M., Fisher, G., Lyon, M.F., 1986. Small eyes (Sey): a homozygous lethal mutation on chromosome 2 which affects the differentiation of both lens and nasal placodes in the mouse. J. Embryol. Exp. Morphol. 97, 95–110.

Jensen, P., Zoghbi, H.Y., Goldowitz, D., 2002. Dissection of the cellular and molecular events that position cerebellar Purkinje cells: a study of the math1 null-mutant mouse. J. Neurosci. 22, 8110–8116.

Jensen, P., Smeyne, R., Goldowitz, D., 2004. Analysis of cerebellar development in math1 null embryos and chimeras. J. Neurosci. 24, 2202–2211.

Karam, S.D., Kim, Y.S., Bothwell, M., 2001. Granule cells migrate within raphes in the developing cerebellum: an evolutionarily conserved morphogenic event. J. Comp. Neurol. 440, 127–135.

Li, S., Goldowitz, D., Swanson, D.J., 2007. The requirement of pax6 for postnatal eye development: evidence from experimental mouse chimeras. Invest. Ophthalmol. Vis. Sci. 48, 3292–3300.

Lin, J.C., Cepko, C.L., 1998. Granule cell raphes and parasagittal domains of Purkinje cells: complementary patterns in the developing chick cerebellum. J. Neurosci. 18, 9342–9353.

Liu, L., Geisert, E.E., Frankfurter, A., Spano, A.J., Jiang, C.X., Yue, J., Dragatsis, I., Goldowitz, D., 2007. A transgenic mouse class-III beta tubulin reporter using yellow fluorescent protein. Genesis 45, 560–569.

Machold, R., Fishell, G., 2005. Math1 is expressed in temporally discrete pools of cerebellar rhombic-lip neural progenitors. Neuron 48, 17–24.

Meech, R., Kallunki, P., Edelman, G.M., Jones, F.S., 1999. A binding site for homeodomain and Pax proteins is necessary for L1 cell adhesion molecule gene expression by Pax-6 and bone morphogenetic proteins. Proc. Natl Acad. Sci. 96, 2420–2425.

Mullen, R.J., Hamre, K.M., Goldowitz, D., 1997. Cerebellar mutant mice and chimeras revisited. Perspect. Dev. Neurobiol. 5, 43–55.

Rakic, P., Sidman, R.L., 1973. Sequence of developmental abnormalities leading to granule cell deficit in cerebellar cortex of weaver mutant mice. J. Comp. Neurol. 152, 103–132.

Reiner, A., Del Mar, N., Deng, Y.P., Meade, C.A., Sun, Z., Goldowitz, D., 2007. R6/2 neurons with intranuclear inclusions survive for prolonged periods in the brains of chimeric mice. J. Comp. Neurol. 505, 603–629.

Ryder, E.F., Cepko, C.L., 1994. Migration patterns of clonally related granule cells and their progenitors in the developing chick cerebellum. Neuron 12, 1011–1028.

Schmahl, W., Knoedlseder, M., Favor, J., Davidson, D., 1993. Defects of neuronal migration and the pathogenesis of cortical malformations are associated with Small eye (Sey) in the mouse, a point mutation at the Pax-6-locus. Acta Neuropathol. 86, 126–135.

Sgaier, S.K., Millet, S., Villanueva, M.P., Berenshteyn, F., Song, C., Joyner, A.L., 2005. Morphogenetic and cellular movements that shape the mouse cerebellum; insights from genetic fate mapping. Neuron 45, 27–40.

Shimada, M., Langman, J., 1970. Repair of the external granular layer after postnatal treatment with 5-fluorodeoxyuridine. Am. J. Anat. 129, 247–259.

Stoykova, A., Gotz, M., Gruss, P., Price, J., 1997. Pax6-dependent regulation of adhesive patterning, R-cadherin expression and boundary formation in developing forebrain. Development 124, 3765–3777.

Sudarov, A., Joyner, A.L., 2007. Cerebellum morphogenesis: the foliation pattern is orchestrated by multi-cellular anchoring centers. Neural Dev. 2, 26.

Swanson, D.J., Tong, Y., Goldowitz, D., 2005. Disruption of cerebellar granule cell development in the Pax6 mutant, Sey mouse. Brain Res. Dev. Brain Res. 16, 176–193.

Takahashi, M., Osumi, N., 2002. Pax6 regulates specification of ventral neurone subtypes in the hindbrain by establishing progenitor domains. Development 129, 1327–1338.

Talamillo, A., Quinn, J.C., Collinson, J.M., Caric, D., Price, D.J., West, J.D., Hill, R.E., 2003. Pax6 regulates regional development and neuronal migration in the cerebral cortex. Dev. Biol. 255, 151–163.

Walther, C., Gruss, P., 1991. Pax-6, a murine paired box gene, is expressed in the developing CNS. Development 113, 1435–1449.

Yamasaki, T., Kawaji, K., Ono, K., Bito, H., Hirano, T., Osumi, N., Kengaku, M., 2001. Pax6 regulates granule cell polarization during parallel fiber formation in the developing cerebellum. Development 128, 3133–3144.

Yang, H., Jensen, P., Goldowitz, D., 2002. The community effect and Purkinje cell migration in the cerebellar cortex: analysis of scrambler chimeric mice. J. Neurosci. 22, 464–470.

Yang, Y., Mufson, E.J., Herrup, K., 2003. Neuronal cell death is preceded by cell cycle events at all stages of Alzheimer's disease. J. Neurosci. 23, 2557–2563.

Yang, Y., Varvel, N.H., Lamb, B.T., Herrup, K., 2006. Ectopic cell cycle events link human Alzheimer's disease and amyloid precursor protein transgenic mouse models. J. Neurosci. 26, 775–784.